The American Journal of Pathology, Vol. 184, No. 10, October 2014

The American Journal of
PATHOLOGY
ajp.amjpathol.org

ANIMAL MODELS

The Impact of Type 1 Diabetes Mellitus on Corneal Epithelial Nerve Morphology and the Corneal Epithelium

Daniel Cai, Meifang Zhu, W. Matthew Petroll, Vindhya Koppaka, and Danielle M. Robertson

From the Department of Ophthalmology, The University of Texas Southwestern Medical Center, Dallas, Texas

Accepted for publication June 17, 2014.

Address correspondence to Danielle M. Robertson, O.D., Ph.D., Department of Ophthalmology, The University of Texas Southwestern Medical Center, 5323 Harry Hines Blvd., Dallas, TX 75390-9057. E-mail: danielle.robertson@utsouthwestern.edu.

Diabetic corneal neuropathy can result in chronic, sight-threatening corneal pathology. Although the exact etiology is unknown, it is believed that a reduction in corneal sensitivity and loss of neurotrophic support contributes to corneal disease. Information regarding the relationship between nerve loss and effects on the corneal epithelium is limited. We investigated changes in the corneal epithelium and nerve morphology using three-dimensional imaging *in vivo* and *in situ* in a streptozotocin-induced diabetic mouse model. Streptozotocin-treated mice showed increased levels of serum glucose and growth retardation consistent with a severe diabetic state. A reduction in the length of the subbasal nerve plexus was evident after 6 weeks of disease. Loss of the subbasal nerve plexus was associated with corneal epithelial thinning and a reduction in basal epithelial cell density. In contrast, loss of the terminal epithelial nerves was associated with animal age. Importantly, this is the first rodent model of type 1 diabetes that shows characteristics of corneal epithelial thinning and a reduction in basal epithelial cell density, both previously have been documented in humans with diabetic corneal neuropathy. These findings indicate that in type 1 diabetes, nerve fiber damage is evident in the subbasal nerve plexus before terminal epithelial nerve loss and that neurotrophic support from both the subbasal nerve plexus and terminal epithelial nerves is essential for the maintenance of corneal epithelial homeostasis. *(Am J Pathol 2014, 184: 2662–2670; http://dx.doi.org/10.1016/j.ajpath.2014.06.016)*

Diabetes mellitus (DM) is a severe metabolic disease with increasing prevalence worldwide. Diabetic neuropathy is one of the most common complications in DM and increases in incidence with both age and duration of disease.[1] At the ocular surface, loss of corneal innervation in DM is associated with reduced corneal sensitivity and altered tear secretion.[2–4] Reduced aqueous tear production from decreased lacrimal gland innervation and an abnormal blink reflex contribute to the high incidence of dry eye that frequently is encountered clinically. In addition, loss of trophic support, which is essential for homeostasis of the epithelium, is believed to contribute to epithelial fragility, corneal erosions, and persistent epithelial defects.[5] Changes in corneal thickness also have been reported. In the earlier stages of disease, central corneal thickening occurs as a result of endothelial dysfunction and increased corneal edema.[6,7] Later stages of disease, however, result in thinning of the corneal epithelium, which is associated with a more severe neurotrophic state.[8] Restoration of corneal epithelial homeostasis and the associated corneal nerve plexus presents an important clinical challenge because many of these neurotrophic conditions are highly refractory to conventional therapies.

In vivo confocal microscopy (IVCM) is used increasingly in clinical studies to evaluate disease-related changes in the subbasal nerve plexus (SBNP). In diabetes, morphologic alterations in the SBNP have been associated with both retinopathy and peripheral neuropathy.[9–12] Although rapid and noninvasive, the use of confocal microscopy in clinical studies prohibits examination of the terminal epithelial nerves (TENs) and raises many questions regarding whether the loss documented by the confocal examination represents one or more fibers, and the type of fibers affected.[13] To address this gap, immunohistochemical studies using rodent models of diabetes have investigated the effects of

Supported in part by NIH grants R01 EY018219 (D.M.R.), R01 EY013322 (W.M.P.), Core grant EY020799, OneSight Research Foundation (D.M.R.), a Career Development Award (D.M.R.), and an unrestricted grant from Research to Prevent Blindness, Inc.

Disclosures: None declared.

Copyright © 2014 American Society for Investigative Pathology.
Published by Elsevier Inc. All rights reserved.
http://dx.doi.org/10.1016/j.ajpath.2014.06.016

hyperglycemia on the SBNP and TENs. By using two-dimensional imaging techniques, these studies have reported reductions in both the SBNP and TENs, with early loss of TENs preceding SBNP damage.[14] However, because of the tortuosity and complex branching patterns of the TENs as they run throughout the corneal epithelium, analysis of TENs from two-dimensional data sets limit the data that can be extracted and therefore requires more advanced three-dimensional (3D) modeling. Moreover, none of the rodent studies to date have shown a detectable effect on central corneal epithelial thickness or basal epithelial cell density (BECD), as seen in humans, as a consequence of disease state or nerve loss.[14,15]

Here, we investigated the effects of type 1 DM on the mouse corneal epithelium. Our primary objective was to evaluate the effects of type 1 DM on total corneal and sublayer thickness and BECD.[16,17] Our secondary objective was to assess the corresponding effects on the neural architecture using 3D volumetric reconstruction of the SBNP and TENs *in situ*. This allowed for a systematic evaluation of corneal nerve thickness and cellular changes in response to disease duration and animal age.

Materials and Methods

Animals

Thirty-one 6-week-old C57/BL6 male mice purchased from the Mouse Breeding Core Facility at The University of Texas Southwestern Medical Center were used in this study. The high-dose streptozotocin (STZ) induction protocol from the Animal Models of Diabetic Complications Consortium was used to induce a type 1 diabetic state, as approved by the University Institutional Animal Care and Use Committee. Briefly, fasting mice underwent a single i.p. injection with 150 mg/kg STZ (Sigma, St. Louis, MO) in citrate buffer, pH 4.5. Mice were subjected to a 4-hour fast before injection. Age-matched control mice were injected with citrate buffer alone. Before treatment, mice were weighed and serum glucose measurements were obtained. For serum glucose determination, blood was sampled from the tip of the tail vein using a OneTouch Ultra Mini glucose monitor (LifeScan, Milpitas, CA). Diabetes was confirmed by day 3. All serum glucose measurements were performed after a minimum fasting time of 5 hours. A fasting serum glucose reading greater than 300 mg/dL was considered diabetic. All control mice remained normoglycemic. On the day of the injection, mice were provided with 10% sucrose water to prevent sudden hypoglycemia. Mice were assessed for body weight, serum glucose level, and corneal changes after either 6 or 12 weeks of hyperglycemia, which corresponded to animal ages of 12 and 18 weeks, respectively. Before enucleation, mice were euthanized under anesthesia by cervical dislocation. All animals were treated according to the Association for Research in Vision and Ophthalmology statement for the use of animals in ophthalmic and vision research.

IVCM

IVCM was performed using a modified Heidelberg Retina Tomograph Rostock Corneal Module (Heidelberg, Germany).[16,17] Before scanning, mice were anesthetized with a single injection of 50 mg/kg ketamine and 5 mg/kg xylazine and one drop of topical proparacaine 0.5% ophthalmic solution (Bausch & Lomb, Tampa, FL). Lubrication was maintained on the contralateral eye using Refresh Plus (Allergan, Irvine, CA). To enhance epithelial viewing, a silicon washer was placed on the outer edge of the TomoCap (Heidelberg, Germany) to generate a thin layer of space between the TomoCap tip and the surface epithelium.[17] The dimensions of the washer were as follows: 1.2-cm outer diameter, 3-mm inner diameter, and 600-μm thick (Specialty Silicone Products, Inc., Ballston Spa, NY). Image acquisition was performed as previously described.[17] Corneas were scanned at a lens speed of 30 μm per second with 1-μm increment steps. A minimum of three scans was performed on each cornea.

Immunofluorescence

Whole globes were removed and incubated in 1.5 mg/mL Dispase (Gibco, Grand Island, NY) in phosphate-buffered saline (PBS) for 2 hours at room temperature with gentle agitation. Corneas were excised and fixed immediately in RNase-free 4% paraformaldehyde (Electron Microscopy Sciences, Fort Washington, PA) in PBS for 40 minutes at room temperature. After washing with PBS, corneal tissue was permeabilized and blocked with 1% bovine serum albumin and 0.2% Triton X-100 (Sigma, St. Louis, MO) in PBS for 2 hours at room temperature. Corneal nerves then were stained with 3.3 μg/mL neuronal class III β-tubulin rabbit polyclonal antibody (MRB-435P; Covance, Emeryville, CA) in 1% bovine serum albumin and 0.2% Triton X-100 in PBS overnight at 4°C. After washing, corneas were incubated in 6.7 μg/mL fluorescein isothiocyanate–conjugated secondary antibody (Alexa488; Cell Signaling, Danvers, MA) with 0.5% bovine serum albumin and 0.1% Triton X-100 in PBS for 2.5 hours at room temperature. Propidium iodide (5 μg/mL; Invitrogen, Grand Island, NY) was added to counterstain epithelial cell nuclei for the final hour. Corneas were mounted on glass-bottom tissue culture dishes (MatTek, Ashland, MA) using a 75% vol/vol solution of glycerol–PBS and imaged on a Leica SP2 laser scanning confocal microscope (Leica Microsystems, Heidelberg, Germany). For each cornea, a single 20× image magnification was acquired to evaluate the overall distribution of the SBNP. By using a 63× water objective, three representative images were acquired at an image zoom of 2.0 for subsequent image processing and analysis.

Image Analysis

Corneal changes *in vivo* were assessed using IVCM. Measurements of total corneal, epithelial, and stromal thickness

values were determined using our in-house confocal microscopy through focusing program.[17] For *in situ* morphologic measurements, data sets were obtained using a laser scanning confocal microscope and used to generate 3D image stacks. To measure BECD from the 63× image stacks, propidium-iodide–stained nuclei within the basal epithelial cell layer were counted manually using MetaMorph software version 7.7.0.0 (Molecular Devices, Inc., Sunnyvale, CA). The total nerve fiber length of the SBNP and TENs was determined using Imaris software version 7.3.1 (BitPlane AG, South Windsor, CT). Within Imaris, surface renderings were generated to model the corneal epithelium and corneal nerves in three dimensions. The FilamentTracer function then was used to trace all subbasal nerve fibers and TENs. This allowed for a combination of automated analysis as well as operator decision to generate a model most representative of the nerve plexus. The SBNP and TENs were analyzed separately. Once the volume renderings were complete, the software program automatically quantified the total length of the nerve fibers from the SBNP and TENs from the resultant 3D models. All measurements were performed by a masked observer (D.C.).

Statistics

Statistical analysis was performed using SigmaPlot 11.0 (Systat Software, Inc., San Jose, CA). All data were expressed as means ± SD. For comparisons between two groups, the Student's *t*-test was used to determine which groups were significantly different. For non-normal distributions, a Mann-Whitney rank-sum test was used. To analyze the effects of multiple factors, a two-way analysis of variance was used. To determine relationships between variables, a Pearson product moment correlation coefficient was determined. Statistical significance was set at $P < 0.05$.

Results

Effects of STZ-Induced Type 1 Diabetes on Body Weight and Serum Glucose Levels

All mice injected with STZ failed to gain weight compared with the vehicle-injected controls. At 12 weeks, the control animals had an increase of 25.8% in body weight when compared with diabetic mice (Figure 1A). Similarly, at 18 weeks, body weight was increased 29.2% in control mice, with no increase over baseline in diabetic animals (Figure 1B). Consistent with failure to thrive, all STZ-treated mice showed observable growth reduction compared with age-matched controls. There was no statistical difference in body weight between STZ-injected mice and vehicle-treated controls at baseline. In contrast to body weight, analysis of serum glucose levels confirmed a significant increase in the STZ-treated mice. There was a 194.4% increase in serum glucose level in the STZ-treated mice at 12 weeks compared with controls (Figure 1C). There was a further 210.5% increase in serum glucose level at 18 weeks in STZ-treated mice over controls (Figure 1D). There was no statistical difference between either group at baseline.

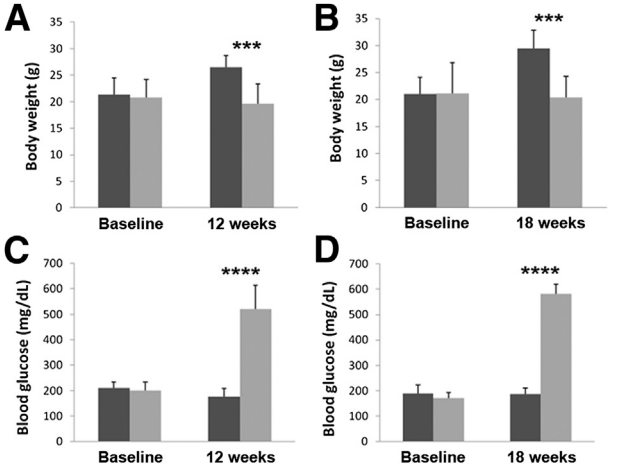

Figure 1 Measurements of body weight and serum glucose level in STZ-treated mice. Body weight was reduced significantly in the STZ-treated group (light gray) compared with the vehicle-treated controls (dark gray) at 12 weeks ($n = 6$) (**A**) and at 18 weeks ($n = 8$) (**B**). There were no differences between the groups at baseline. Serum glucose level was increased significantly at 12 weeks ($n = 6$) (**C**) and at 18 weeks ($n = 8$) (**D**) in the STZ-treated groups compared with the vehicle-treated controls. There were no differences in serum glucose level at baseline in either group. Data are expressed as means ± SD. ***$P < 0.001$, ****$P < 0.0001$.

Effects of Type 1 Diabetes on the Corneal Epithelium

The effects of type 1 diabetes on the full-thickness mouse cornea and surface epithelium was evaluated using IVCM. Representative images are shown in Figure 2 and Supplemental Video S1. After 12 weeks of STZ-induced diabetes, there was a 7.2% reduction in total corneal thickness; however, this finding was not significant (Table 1). An analysis of the sublayer corneal thickness showed that this effect was mediated by a decrease in stromal thickness (10.2% thinner in the STZ-treated group compared with controls) whereas there was only a 1.6% reduction in thickness of the corneal epithelium. At 18 weeks of disease, the total corneal thickness was reduced significantly by 10.2% in STZ-treated mice compared with controls ($P = 0.011$). In contrast to 12 weeks, this was accompanied by significant thinning of the corneal epithelium (12.2% reduction compared with controls; $P = 0.026$). Although not significant, stromal thickness in this group decreased similarly by 9.3%.

Double-labeling of corneal nerves and epithelial nuclei allowed for an assessment of epithelial perturbations in the normal and diseased states (Figure 3, A–C). Of note, BECD was decreased significantly in the corneal epithelium of diabetic mice. There was a 6.3% reduction at 12 weeks (Figure 3D) ($P = 0.011$) and a 4.5% reduction at 18 weeks (Figure 3E) ($P = 0.012$). Comparison of the right and left

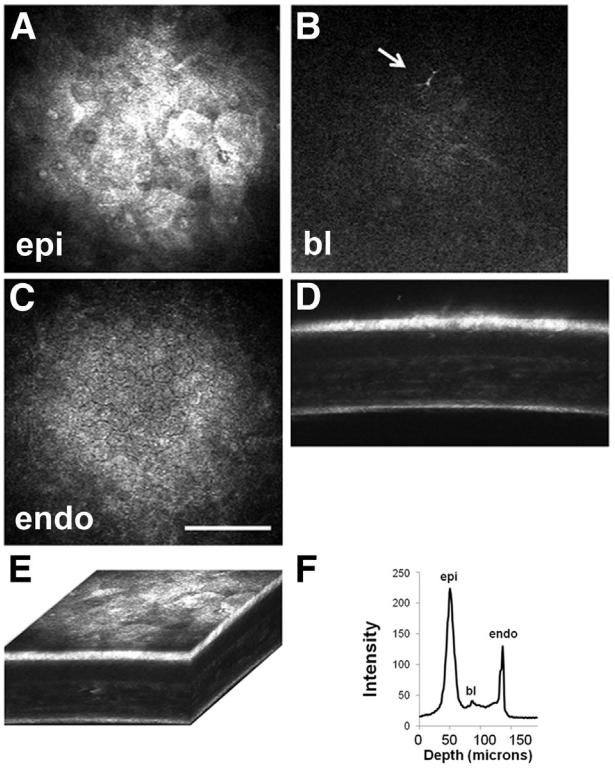

Figure 2 Quantitative 3D *in vivo* confocal microscopy. Representative images showing the surface epithelium (**A**), the basal lamina with subbasal nerve plexus (SBNP) (**B**), and the endothelium (**C**). **B:** Note the presence of an infiltrated dendritic cell (**arrow**). **D:** An *X-Z* projection shows all corneal layers. **E:** Three-dimensional rendering of the full-thickness cornea. **F:** Intensity profile generated from backscattered light allows the determination of total and sublayer thickness. Scale bar = 100 μm (**C**). bl, basal lamina; endo, endothelium; epi, epithelium.

eyes of individual mice showed no significant difference in BECD.

Effects of Type 1 Diabetes on the Subbasal Plexus and TENs

From the 3D volumetric images, three different nerve morphologies were observed: simple, ramifying, and complex. Representative images are shown in Figure 4. Simple TENs were identified as branching from the SBNP and projecting anteriorly toward the corneal surface (Figure 4, A and B). Similar to simple nerves, ramifying nerves branched from the SBNP and ran anteriorly toward the corneal surface. However, ramifying nerves underwent subsequent branching within either the wing or squamous epithelial cell layers, and continued to course parallel to the SBNP (Figure 4, C and D) throughout superficial cell layers. The length of these parallel fibers varied greatly and often spanned distances of >3 to 5 epithelial cells in length. In contrast to simple and ramifying nerves, complex TENs showed a multibranching pattern among wing and surface epithelial cells (Figure 4, E and F), with evidence of anastomoses detected between more apically localized nerve fibers (not shown).

Low-magnification views of the SBNP showed visible nerve fiber degradation with patchy regions of nerve fiber loss in the diabetic cornea compared with the vehicle-treated control, including focal loss within the whorl-like vortex (Figure 5, A and B). Within the patchy areas of SBNP damage, the overall length of the TENs seen branching from the remaining subbasal nerve fibers appeared relatively unchanged. Representative 3D renderings and segmentation of the SBNP and TENs generated in normal and diabetic corneas are shown in Figure 5, C–F and in Supplemental Videos S2, S3, S4, and S5. Only a small proportion of subbasal nerve fibers showed evidence of TEN branching in the normal cornea. In contrast, in the diabetic cornea, there were fewer nonbranching fibers observed.

To investigate quantitative changes in the SBNP and TENs, the total length of the SBNP and TENs were calculated independently using Imaris. By using this method, we found a significant reduction in total nerve fiber length in the SBNP in diabetic mice compared with controls ($P < 0.001$ at 12 and 18 weeks, respectively). This decrease was more pronounced at 18 weeks, which showed a 40.5% reduction in length compared with a 31% reduction at 12 weeks (Figure 6A). The interaction between disease and animal age was significant ($P = 0.046$). In contrast to the SBNP, there was only a small difference between the diabetic and control groups in TEN length at either 12 or 18 weeks (Figure 6B) ($P = 0.034$). However, there was an obvious reduction in TEN length in both the diabetic and control groups at 18 weeks compared with 12 weeks (Figure 6B) ($P < 0.001$). There was no interaction between animal age and disease ($P = 0.860$). Similar to the TENs, there was no interaction between age and disease for BECD ($P = 0.359$). There was no significant difference in the length of the SBNP, TENs, or BECD between the left and right eyes. Significant correlations were found among all three outcome measures (Figure 7). The weakest correlation was between TENs and the SBNP ($r = 0.35$, $P = 0.005$). Moderate correlations were seen between BECD and TENs ($r = 0.40$, $P = 0.002$) and BECD and SBNP ($r = 0.44$, $P = 0.0004$).

Table 1 Summary of Corneal Thickness Values

Animal age	STZ-treated group (μm)	Vehicle-only control (μm)	*P* value
12 weeks			
Total corneal thickness	98.3 ± 14.1	105.9 ± 13.6	0.291
Epithelial thickness	36.8 ± 5.1	37.4 ± 6.5	0.834
Stromal thickness	61.5 ± 9.4	68.5 ± 9.1	0.156
18 weeks			
Total corneal thickness	97.6 ± 8.5	108.7 ± 4.8	0.011*
Epithelial thickness	34.0 ± 3.0	38.6 ± 3.8	0.026*
Stromal thickness	63.6 ± 7.2	70.1 ± 5.5	0.085

Corneal thickness values are means ± SD.
*$P < 0.05$.

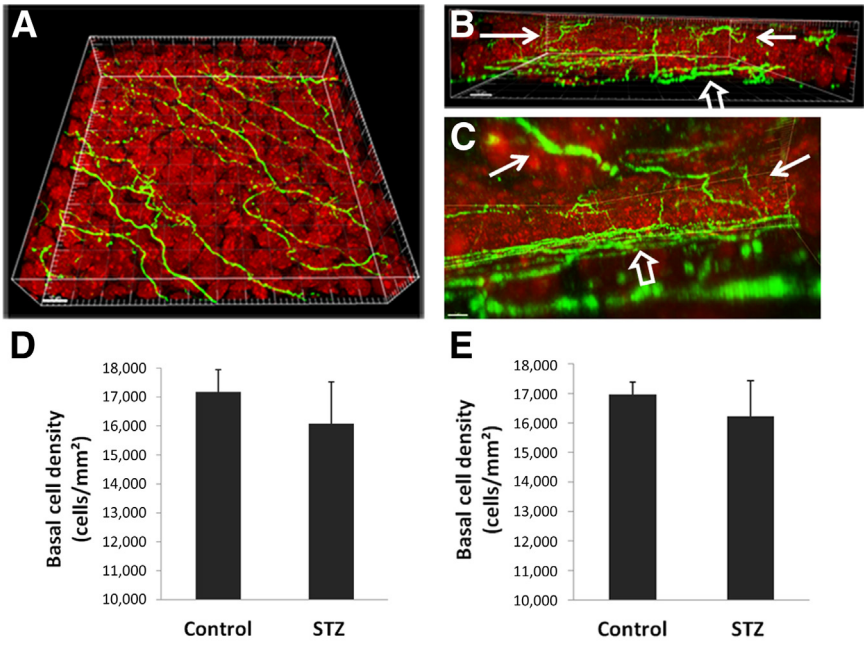

Figure 3 Three-dimensional reconstruction of the corneal epithelium and associated epithelial nerves. Corneal nerves were labeled with neuronal βIII tubulin (green) and nuclei were counterstained with propidium iodide (red, 63×). **A:** Three-dimensional surface-rendering view from the apical surface shows the spatial distribution of the subbasal nerve plexus (SBNP). **B:** The view from the side shows the terminal epithelial nerves (TEN)s. **C:** The view from within the corneal epithelium shows the branching patterns and interconnections among TENs (**solid arrows** indicate TENs, **open arrows** indicate the SBNP). **D** and **E:** The mean density of basal epithelial cells was reduced significantly in the streptozotocin (STZ)-treated animals compared with vehicle-treated controls at both 12 weeks ($P = 0.011$, $n = 8$ for both STZ and control groups) (**D**) and 18 weeks ($P = 0.012$, $n = 8$ for both STZ and control groups) (**E**). Data are representative of means ± SD. Scale bars: 8 μm (**A**–**C**).

Discussion

There were two significant findings in this study. First, the central corneal thickness was reduced in the severely diabetic state. The reduction in corneal thickness was evident at both the stroma and epithelium levels. Clinically, changes in corneal thickness have been reported previously in diabetes.[6–8] By using tandem scanning confocal microscopy, Rosenberg et al[8] reported epithelial thinning in patients with significant corneal neuropathy. However, they reported an increase in stromal thickness caused by corneal edema. Here, we found that stromal thickness was reduced at both disease time points and was associated with significant growth retardation in the diabetic state. This finding suggests that the widespread effects of hyperglycemia may impact and/or disrupt stromal development. Although not investigated here, stromal biomechanical properties have been reported to be altered in diabetes. These include an

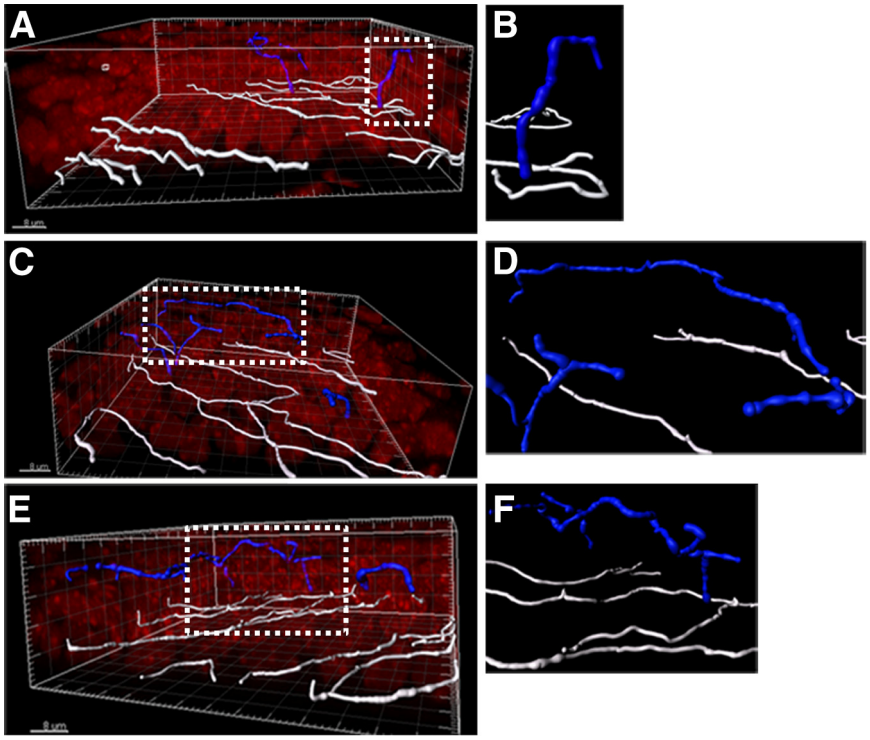

Figure 4 Morphology of terminal epithelial nerves (TEN). Three-dimensional surface renderings of the subbasal nerve plexus (white) and TENs (blue). Propidium iodide–stained nuclei are shown in red. Short simple nerve (**A** and **B**), long simple nerve (**C** and **D**), and a complex nerve (**E** and **F**) are shown. **B**, **D**, and **F:** Corresponding zoomed regions from **A**, **C**, and **E**, respectively, as indicated by the **dotted box**. Scale bars: 8 μm (**A**, **C**, and **E**).

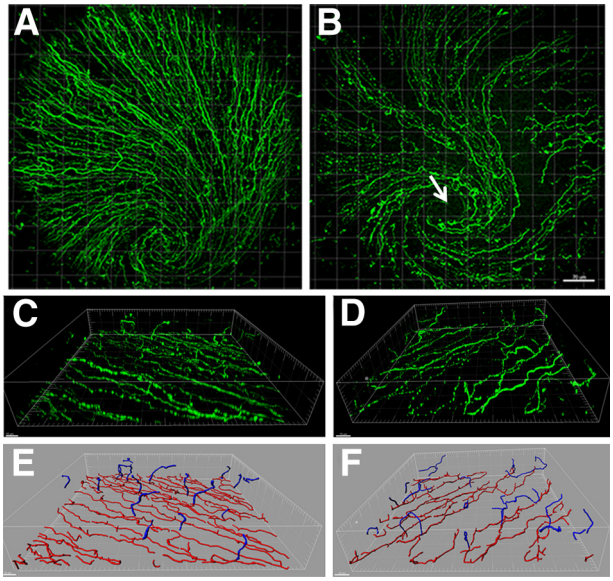

Figure 5 Distribution of loss in the subbasal nerve plexus (SBNP). Representative 20× images of neuronal βIII tubulin–stained nerves of the full SBNP in control (**A**) and 18-week streptozotocin-treated (**B**) corneas. Note both diffuse nerve loss with patchy focal areas of dropout. **B: Arrow** indicates the damage at the area of the whorl. **C** and **D:** Three-dimensional surface rendering of the SBNP and terminal epithelial nerves (TEN) in normal (**C**) and diabetic (**D**) corneas. Three-dimensional nerve modeling and segmentation using Imaris Filament. **E** and **F:** The SBNP is shown in red and TENs are shown in blue. Normal SBNP and TENs (**E**), diabetic SBNP and TENs (**F**). Scale bars: 70 μm (**B**);10 μm (**C** and **D**).

increase in corneal hysteresis, which has been postulated to be caused by increased accumulation of advanced glycation end products, and abnormalities in collagen organization.[18] The role of chronic hyperglycemic stress on keratocyte function and the downstream impact on stromal remodeling represents an important avenue of future research.

In contrast to the stroma, central epithelial thinning was present only in the diabetic animals. We also reported a slight, but significant, decrease in BECD within the central and paracentral corneal epithelium. This decrease was similar to an earlier report by Chang et al[19] that showed a reduction in BECD in humans with diabetic retinopathy. In agreement with that study, the reduction in BECD paralleled the loss of the SBNP. This change in BECD, coupled with corneal epithelial thinning, indicates a disruption in the normal homeostasis of the corneal epithelium. Although it is unknown whether corneal epithelial changes in diabetes are driven directly by a loss of neurotrophic support from the SBNP or indirectly through alterations in corneal sensitivity and the blink reflex,[20] the findings from the present study suggest a partial contributory component for both.

It is well-established clinically that ocular surface inflammation and dry eye are associated frequently with diabetes.[21,22] This is caused in part by direct hyperglycemia-mediated damage to the lacrimal gland.[23–25] Because dry eye is accompanied by an increase in apoptotic-driven surface cell desquamation,[26] a potential increase in epithelial surface cell loss that is greater than the basal epithelial cell mitotic rate would result in a net thinning of the corneal epithelium, as seen in the diabetic animals. A thinned compromised epithelium that fails to maintain optimal lubrication in the presence of an inadequate blink response predisposes the cornea to an increased risk of surface epithelial damage.[27] Similarly, a disruption in the normal barrier function of the epithelium may contribute to an increased risk of infection, as has been reported previously in the diabetic eye.[28–30]

In the absence of disease, murine corneal thickness values have been reported to increase during the first 4 to 8 weeks of postnatal life, leveling off and remaining relatively unchanged throughout adulthood.[31] Previous studies have investigated central corneal and epithelial thickness in the C57/BL6 mouse cornea. Henriksson et al[32] used conventional light microcopy of glutaraldehyde-fixed tissue *in situ* and reported a mean central corneal thickness of 137.02 μm with measurements of 40.59 and 90.88 μm for the

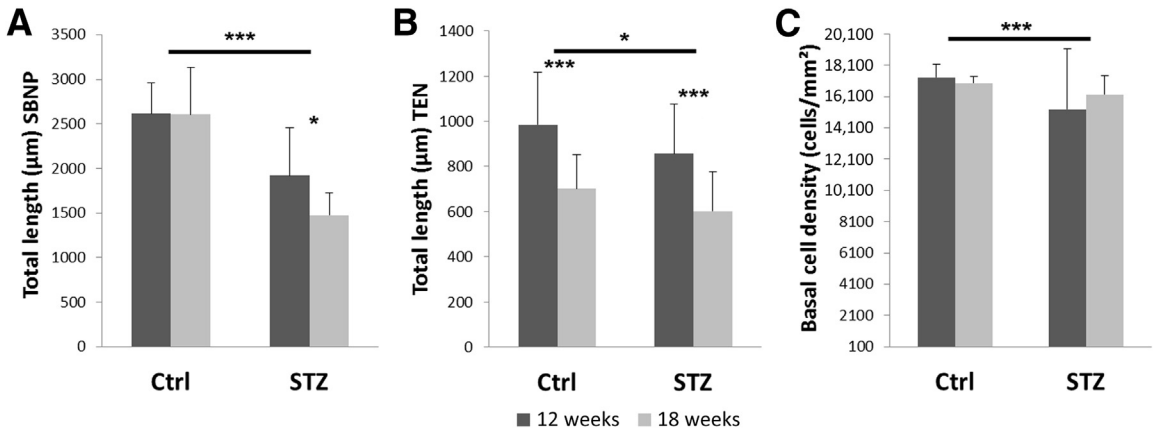

Figure 6 Effects of age and disease on the subbasal nerve plexus (SBNP) and terminal epithelial nerves (TEN). **A:** Length of the SBNP was reduced significantly as a consequence of disease; however, longer disease duration was associated with greater loss (age, $P = 0.041$; interaction, $P = 0.046$). **B:** In contrast, TEN length was affected minimally by animal age, and was not dependent on health status (health, $P = 0.034$; interaction, $P = 0.860$). **C:** There was a significant difference in basal epithelial cell density as a function of disease, which was not influenced by age or interaction (age, $P = 0.638$; interaction, $P = 0.359$). Data are representative of means ± SD. $*P < 0.05$, $***P < 0.001$. Ctrl, control.

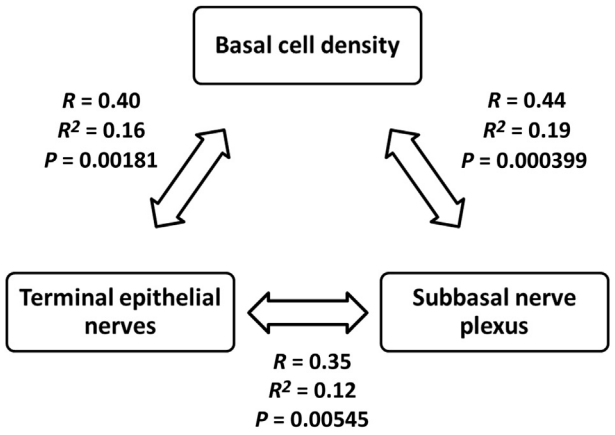

Figure 7 Relationship between subbasal nerve plexus (SBNP), terminal epithelial nerves (TEN), and basal epithelial cell density (BECD). There was a moderate correlation between changes in the SBNP and a reduction in BECD ($R = 0.44$, $P = 0.000399$) and between TENs and BECD ($R = 0.40$, $P = 0.00181$). Loss of TEN was correlated only weakly with loss of the SBNP ($R = 0.35$, $P = 0.00545$).

epithelium and stroma, respectively. More recently, Zhang et al[33] used two-photon imaging to assess corneal thickness *in vivo* in C57/BL6 mice and found central values of 116.6, 39.9, and 76.7 μm for total, epithelial, and stromal thicknesses, respectively. Spectral domain optical coherence tomography also has been used to assess corneal thickness *in vivo* and *in situ*.[31] In this study, the investigators reported a central corneal thickness value of 106 μm for adult mice *in vivo* compared with 141 μm for fixed tissue *in situ*. Because of limitations when using optical coherence tomography, sublayer thickness values were not reported. Here, total corneal thickness values in control mice measured 105.9 ± 13.6 μm and 108.7 ± 4.8 μm using IVCM, at approximately 12 and 18 weeks of age, respectively. These findings are in agreement with the previous *in vivo* optical coherence tomography reports and support the use of IVCM for corneal thickness determination in this study.

To date, all other studies evaluating corneal thickness in STZ-treated rat models have reported that corneal thickness is unchanged in diabetic animals compared with normal controls.[14,15] This could be a result of variability in the rat corneal response compared with the mouse, differences in the STZ procedure used, or a limitation of the imaging system. In their study using STZ-treated Sprague-Dawley rats, Yin et al[15] used the ConfoScan (Nidek, Fremont, CA) to evaluate corneal thickness after a disease duration of 8 weeks. They reported an average corneal thickness of 170 μm, which was unchanged as a consequence of diabetes. However, because of the lack of applanation and lower axial resolution of the ConfoScan, it is possible that the instrument was unable to detect small differences in corneal thickness between the test and control groups. Davidson et al[14] also evaluated corneal thickness in Sprague-Dawley rats after 8 weeks of diabetes. In their study, measurements were obtained using the Heidelberg Retina Tomograph confocal microscope. The mean corneal thickness was reported as 137 μm in control rats, 126 μm in diabetic animals, and 121 μm in diabetic animals receiving treatment for their disease. Although this decrease was not statistically significant, it still represents an 8% reduction in total corneal thickness in the diabetic rodent cornea, which is consistent with our results.

The second key finding in this study was that a reduction in the total length of the SBNP was associated with hyperglycemia, whereas a decrease in the TENs occurred as a consequence of normal maturation. The loss of SBNP in response to prolonged hyperglycemia is in agreement with previous rodent and human clinical models.[8–12,15,27,34] This response was greatest at 18 weeks and is consistent with duration of disease as a risk factor for diabetic neuropathy.[1] Multiple mechanisms have been proposed to play a role in the onset and progression of diabetic neuropathy. These include hyperglycemia-induced inflammation and oxidative stress, altered metabolic and signaling pathways, and vascular insufficiency. In the cornea, a reduction in acetylcholine-mediated vascular relaxation of the posterior ciliary artery has been shown to be associated with decreasing nerve fiber length in the SBNP.[35] Thus, in addition to locally derived mediators, systemic factors associated with diabetes may play a significant role in the deterioration of the SBNP. This has been supported by clinical studies that showed that reductions in systemic risk factors associated with diabetes as well as successful pancreas transplantation are associated with an enhancement in SBNP morphology.[11,36,37]

Earlier findings by Davidson et al[14] using two-dimensional corneal imaging reported that the TENs in the diabetic rodent are lost before any detectable damage occurs in the SBNP. Here, although we did see changes at the whorl-like vortex that accompanied patchy loss of the SBNP,[38] we were unable to detect an early loss or degradation of the TENs before the SBNP changes. Instead, we observed fewer nonbranching fibers within the SBNP in the diabetic cornea when compared with controls. Although we recognize that the small field of view in the high-magnification image prohibits the ability to follow the nonbranching nerves over longer distances, the observation that nonbranching nerves may be lost first would indicate that robust SBNP loss is required before substantial effects on the TENs would be seen. Because terminal corneal nerve fibers are responsible for relaying nociceptive sensory input, a decrease in TENs would be required before a loss in corneal sensitivity.[39] This would explain findings by Yin et al,[15] who reported only a modest correlation between changes in the SBNP and corneal sensitivity, as measured by corneal touch thresholds, in their STZ-treated rat model. Indeed, this hypothesis also is consistent with clinical data showing that early changes in the SBNP are not associated with loss of corneal sensation but that damage of a much greater magnitude is required.[8]

Length of the TENs was reduced in older animals independent of disease. This age-related effect was not evident at the level of the SBNP. The finding of an age-related loss in TENs is consistent with a previous study evaluating

age-related changes in the mouse cornea.[40] In that study, the investigators showed that corneal nerve terminal density increased from postnatal day 1 until 8 weeks, with a gradual reduction onward. This natural pruning of TENs in the cornea may reflect normal age-related remodeling of the TENs. Additional studies using older animals are required to examine the contributory relationship between loss of the TENs, corneal sensitivity, and lacrimal input.

Although immunofluorescent studies permit analysis of the corneal TEN architecture, which is beyond the current resolution limits of the confocal microscope *in vivo*, there were limitations to this technique. Specifically, the presence of any background fluorescence within the image can induce image artifacts and result in the appearance of nerve fibers that may not be present. This factor was controlled for in the current study by using a combination of automatic and manual nerve fiber tracings to allow for optimal reproduction of the nerves in the 3D models. A second potential limitation to the present study was in the regional nature of nerve fiber loss within the SBNP. Because three predefined regions were selected for imaging in all samples, this resulted in increased variability in the data set. The use of three predetermined regions, however, was essential to control for any investigator bias in region selection during imaging.

Conclusions

This is the first rodent model of type 1 diabetes that shows corneal epithelial thinning and changes in BECD associated with diabetic corneal neuropathy that parallel changes reported in humans. These findings indicate that the pathophysiological effects of hyperglycemia impact SBNP before TEN loss and that neurotrophic support from both SBNP and TENs is essential for the maintenance of corneal epithelial homeostasis. Because changes in the corneal nerve architecture and corneal sensitivity increasingly are being implemented as outcome measures in studies evaluating disease severity, comorbidity, and therapeutic modalities in diabetes, it is imperative to elucidate the pathophysiological mechanisms that underlie these changes. Further studies that incorporate the use of human donor corneal tissue to investigate these changes systematically are required to confirm and extend these findings.

Supplemental Data

Supplemental material for this article can be found at *http://dx.doi.org/10.1016/j.ajpath.2014.06.016*.

References

1. Boulton AJ, Malik RA, Arezzo JC, Sosenko JM: Diabetic somatic neuropathies. Diabetes Care 2004, 27:1458–1486
2. Cousen P, Cackett P, Bennett H, Swa K, Dhillon B: Tear production and corneal sensitivity in diabetes. J Diabetes Complications 2007, 21: 371–373
3. Dogru M, Katakami C, Inoue M: Tear function and ocular surface changes in noninsulin-dependent diabetes mellitus. Ophthalmology 2001, 108:586–592
4. Goebbels M: Tear secretion and tear film function in insulin dependent diabetics. Br J Ophthalmol 2000, 84:19–21
5. Wu Y-C, Buckner BR, Zhu M, Cavanagh HD, Robertson DM: Elevated IGFBP3 levels in diabetic tears: a negative regulator of IGF-1 signaling in the corneal epithelium. Ocul Surf 2012, 10:100–107
6. Busted N, Olsen T, Schmitz O: Clinical observations on the corneal thickness and the corneal endothelium in diabetes mellitus. Br J Ophthalmol 1981, 65:687–690
7. Lee JS, Oum BS, Choi HY, Lee JE, Cho BM: Differences in corneal thickness and corneal endothelium related to duration in diabetes. Eye (Lond) 2006, 20:315–318
8. Rosenberg ME, Tervo TM, Immonen IJ, Muller LJ, Gronhagen-Riska C, Vesaluoma MH: Corneal structure and sensitivity in type 1 diabetes mellitus. Invest Ophthalmol Vis Sci 2000, 41:2915–2921
9. De Cilla S, Ranno S, Carini E, Fogagnolo P, Ceresara G, Orzalesi N, Rossetti LM: Corneal subbasal nerve changes in patients with diabetic retinopathy: an in vivo confocal study. Invest Ophthalmol Vis Sci 2009, 50:5155–5158
10. Nitoda E, Kallinikos P, Pallikaris A, Moschandrea J, Amoiridis G, Ganotakis ES, Tsilimbaris M: Correlation of diabetic retinopathy and corneal neuropathy using confocal microscopy. Curr Eye Res 2012, 37:898–906
11. Tavakoli M, Kallinikos P, Igbal A, Herbert A, Fadavi H, Efron N, Boulton AJ, Malik RA: Corneal confocal microscopy detects improvements in corneal nerve morphology with an improvement in risk factors for diabetic neuropathy. Diabet Med 2011, 28:1261–1267
12. Tavakoli M, Quattrini C, Abbott C, Kallinikos P, Marshall A, Finnigan J, Morgan P, Efron N, Boulton AJ, Malik RA: Corneal confocal microscopy: a novel noninvasive test to diagnose and stratify the severity of human diabetic neuropathy. Diabetes Care 2010, 33:1792–1797
13. Erie JC, McLaren JW, Hodge DO, Bourne WM: The effect of age on the corneal subbasal nerve plexus. Cornea 2005, 24:705–709
14. Davidson EP, Coppey LJ, Yorek MA: Early loss of innervation of corneal epithelium in streptozotocin-induced type 1 diabetic rats: improvement with ilepatril treatment. Invest Ophthalmol Vis Sci 2012, 53:8067–8074
15. Yin J, Huang J, Chen C, Gao N, Wang F, Yu F-SX: Corneal complications in streptozocin-induced type 1 diabetic rats. Invest Ophthalmol Vis Sci 2011, 52:6589–6596
16. Petroll WM, Cavanagh HD: Remote-controlled scanning and automated confocal microscopy through focusing using a modified HRT Rostock corneal module. Eye Contact Lens 2009, 35:302–308
17. Petroll WM, Weaver M, Vaidya S, McCulley JP, Cavanagh HD: Quantitative 3-D corneal imaging in vivo using a modified HRT-RCM confocal microscope. Cornea 2012, 32:e36–e43
18. Scheler A, Spoerl E, Boehm AG: Effect of diabetes mellitus on corneal biomechanics and measurement of intraocular pressure. Acta Ophthalmol 2012, 90:e447–e451
19. Chang P-Y, Carrel H, Huang J-S, Wang I-J, Hou Y-C, Chen W-L, Wang J-Y, Hu F-R: Decreased density of corneal basal epithelium and subbasal corneal nerve bundle changes in patients with diabetic retinopathy. Am J Ophthalmol 2006, 142:488–490
20. Shetty R, Saeed T, Rashed H, Adeghate E, Singh J: Effects of diabetes mellitus on acinar gland morphology, peroxidase concentration, and release in isolated rat lacrimal glands. Curr Eye Res 2009, 34:905–911
21. Kaiserman I, Kaiserman N, Nakar S, Vinker S: Dry eye in diabetic patients. Am J Ophthalmol 2005, 139:498–503
22. Manaviat MR, Rashidi M, Afkhami-Ardekani M, Shoja MR: Prevalence of dry eye syndrome and diabetic retinopathy in type 2 diabetic patients. BMC Ophthalmol 2008, 8:10–14
23. Zagon IS, Klocek MS, Sassani JW, McLaughlin PJ: Dry eye reversal and corneal sensation restoration with topical naltrexone in diabetes mellitus. Arch Ophthalmol 2009, 127:1468–1473
24. Alves MC, Carvalheira JB, Modulo CM, Rocha EM: Tear film and ocular surface changes in diabetes mellitus. Arq Bras Oftamol 2008, 71:96–103

25. Modulo CM, Jorge AG, Dias AC, Braz AM, Bertazolli-Filho R, Jordao AAJ, Sergio Marchini J, Rocha EM: Influence of insulin treatment on the lacrimal gland and ocular surface of diabetic rats. Endocrine 2009, 36:161−168
26. Yeh S, Song XJ, Farley W, Li D-Q, Stern ME, Pflugfelder SC: Apoptosis of ocular surface cells in experimentally induced dry eye. Invest Ophthalmol Vis Sci 2003, 44:124−129
27. Messmer EM, Schmid-Tannwald C, Zapp D, Kampik A: In vivo confocal microscopy of corneal small fiber damage in diabetes mellitus. Graefes Arch Clin Exp Ophthalmol 2010, 248:1307−1312
28. Cho BJ, Lee GJ, Ha SY, Seo YH, Tchah H: Co-infection of the human cornea with Stenotrophomonas maltophilia and Aspergillus fumigatus. Cornea 2002, 21:628−631
29. Holifield K, Lazzaro DR: Case report: spontaneous Stenotrophomonas matlophilia keratitis in a diabetic patient. Eye Contact Lens 2011, 37:326−327
30. Gekka M, Miyata K, Nagai Y, Nemoto S, Sameshima T, Tanabe T, Maruoka S, Nakahara M, Kato S, Amano S: Corneal epithelial barrier function in diabetic patients. Cornea 2004, 23:35−37
31. Hanlon SD, Patel NB, Burns AR: Assessment of postnatal corneal development in the C57BL/6 mouse using spectral domain optical coherence tomography and microwave-assisted histology. Exp Eye Res 2011, 93:363−370
32. Henriksson JT, McDermott AM, Bergmanson JPG: Dimensions and morphology of the cornea in three strains of mice. Invest Ophthalmol Vis Sci 2009, 50:3648−3654
33. Zhang H, Wang L, Xie Y, Liu S, Deng X, He S, Chen G, Liu H, Yang B, Zhang J, Sun S, Li X, Li Z: The measurement of corneal thickness from center to limbus in vivo in C57BL/6 and BALB/c mice using two-photon imaging. Exp Eye Res 2013, 115:255−262
34. Ahmed A, Bril V, Orszag A, Paulson J, Yeung E, Ngo M, Orlov S, Perkins BA: Detection of diabetic sensorimotor polyneuropathy by corneal confocal microscopy in type 1 diabetes: a concurrent validity study. Diabetes Care 2012, 35:821−828
35. Davidson EP, Coppey LJ, Holmes A, Yorek MA: Changes in corneal innervation and sensitivity and acetylcholine-mediated vascular relaxation of the posterior ciliary artery in a type 2 diabetic rat. Invest Ophthalmol Vis Sci 2012, 53:1182−1187
36. Mehra S, Tavakoli M, Kallinikos PA, Efron N, Boulton AJ, Augustine T, Malik RA: Corneal confocal microscopy detects early nerve regeneration after pancreas transplantation in patients with type 1 diabetes. Diabetes Care 2007, 30:2608−2612
37. Tavakoli M, Mitu-Pretorian M, Petropoulos IN, Fadavi H, Asghar O, Alam U, Ponirakis G, Jeziorska M, Marshall A, Efron N, Boulton AJ, Augustine T, Malik RA: Corneal confocal microscopy detects early nerve regeneration in diabetic neuropathy after simultaneous pancreas and kidney transplantation. Diabetes 2013, 62:254−260
38. Davidson EP, Coppey LJ, Kardon RH, Yorek MA: Differences and similarities in development of corneal nerve damage and peripheral neuropathy and in diet-induced obesity and type 2 diabetic rats. Invest Ophthalmol Vis Sci 2014, 55:1222−1230
39. Ivanusic JJ, Wood RJ, Brock JA: Sensory and sympathetic innervation of the mouse and guinea pig corneal epithelium. J Comp Neurol 2013, 521:877−893
40. Wang C, Fu T, Xia C, Li Z: Changes in mouse corneal epithelial innervation with age. Invest Ophthalmol Vis Sci 2012, 53:5077−5084